



Missouri University of Science and Technology
Scholars' Mine

International Specialty Conference on Cold-Formed Steel Structures

(2014) - 22nd International Specialty Conference on Cold-Formed Steel Structures

Nov 6th, 12:00 AM - 12:00 AM

In-Plane Behavior of Cold-Formed Steel-Framed Shear Wall Panels Sheathed with Fibre Cement Board

Rojit Shahi

Nelson Lam

Emad Gad

Ismail Saifullah

John Wilson

See next page for additional authors

Follow this and additional works at: <https://scholarsmine.mst.edu/isccss>

 Part of the [Structural Engineering Commons](#)

Recommended Citation

Shahi, Rojit; Lam, Nelson; Gad, Emad; Saifullah, Ismail; Wilson, John; and Watson, Ken, "In-Plane Behavior of Cold-Formed Steel-Framed Shear Wall Panels Sheathed with Fibre Cement Board" (2014). *International Specialty Conference on Cold-Formed Steel Structures*. 3.

<https://scholarsmine.mst.edu/isccss/22iccfss/session11/3>

This Article - Conference proceedings is brought to you for free and open access by Scholars' Mine. It has been accepted for inclusion in International Specialty Conference on Cold-Formed Steel Structures by an authorized administrator of Scholars' Mine. This work is protected by U. S. Copyright Law. Unauthorized use including reproduction for redistribution requires the permission of the copyright holder. For more information, please contact scholarsmine@mst.edu.

Author

Rojit Shahi, Nelson Lam, Emad Gad, Ismail Saifullah, John Wilson, and Ken Watson

In-Plane Behavior of Cold-Formed Steel-Framed Wall Panels Sheathed with Fibre Cement Board

Rojit Shahi¹, Nelson Lam², Emad Gad³, Ismail Saifullah⁴, John Wilson⁵ & Ken
Watson⁶

Abstract

Shear wall panels are commonly used as lateral load resisting elements to provide stability of the cold-formed steel-framed houses in Australia against wind and earthquake actions. The effectiveness of their lateral resistance behavior is obtained usually by experimental testing although it can also be done by analytical modeling. This paper presents racking test results of steel-framed wall panels with different aspect ratios sheathed with fibre cement board subjected to monotonic and cyclic loading protocol. Performance parameters of the wall panels are obtained from the experimentally observed load-deflection curves using various existing methods and evaluation method is proposed. The evaluation method considers various performance characteristics including ductility modification factor, residual displacement recovery and load levels satisfying ultimate and serviceability limit state conditions.

¹ PhD Research Student, Department of Infrastructure Engineering, The University of Melbourne, Parkville, VIC, Australia

² Associate Professor and Reader, Department of Infrastructure Engineering, The University of Melbourne, Parkville, VIC, Australia

³ Professor, Department of Civil and Construction Engineering, Swinburne University of Technology, Hawthorn, VIC, Australia

⁴ PhD Research Student, Department of Civil and Construction Engineering, Swinburne University of Technology, Hawthorn, VIC, Australia

⁵ Executive Dean, Faculty of Science, Engineering and Technology, Swinburne University of Technology, Hawthorn, VIC, Australia

⁶ Executive Director, National Association of Steel-Framed Housing Inc (NASH), VIC, Australia

1. Introduction

Cold-formed steel (CFS) has been widely used in domestic low-rise buildings in industrialized countries including Australia. Commonly, shear wall panels are the main vertical elements for resisting lateral loads (due to wind or earthquake) in this type of construction. A typical shear wall panel consists of a CFS frame that is composed of studs, top & bottom plates and noggings; and sheathing panels. Top and bottom plates are connected to the studs to form the frame and the sheathing panel is connected to the frame by discrete fasteners. Racking strength and stiffness of a shear wall panel is primarily governed by the connections between the sheathing and the frame, also termed as sheathing-to-framing connections. Shear wall panels under lateral loading exhibit very complex and high nonlinear behavior which is mainly attributed to the nonlinear behavior of the sheathing-to-framing connections. Due to its highly nonlinear behavior, determination of definite yield point from the observed load-deflection backbone curve is not convenient as in the cases of other conventional material/system. This leads to diverse values of wall parameters to be obtained based on the assumptions made in determining the yield point. Not only is the performance of the wall dependent on the evaluation method, but also dependent largely on the loading protocol used in the experimental testing (Gatto & Uang 2003). Whilst numerous loading protocols exist for the cyclic testing of structures, a new loading protocol (Shahi *et al.* 2013) which had been recently developed based on the seismic conditions of Australia (AS 1170.4:2007), is used in this study for cyclic testing.

2. Experimental Program

Experimental studies were carried out on two different lengths (shown in Table 1) of wall panels braced with fibre cement boards. The wall panels were built from CFS framing members and fibre cement sheathing panels. The CFS frame was made of 89x36x0.75mm C-shaped lipped studs (with web stiffened) and 91x40x0.75mm plain channel sections for plates and noggings. Studs were placed at 600mm spacings for 2.4m long wall and 450mm spacings for 0.9m long wall. Two identical fibre cement boards of 5mm thickness were used as the sheathing boards for Wall Panel A whereas one board of 5mm thickness was used for Wall Panel B. The sheathing boards were attached vertically on one face of the wall panel. For tie-down of the wall panel at the floor level, M12 hold-down bolts with 50 x 50 x 3mm distribution washers were used at the two outside frame studs whereas M8 hold-down bolts with 32mm diameter 2.5mm thick round washers were used at the interior studs. All bolts were placed within 45mm from the web of the studs. An additional end restraint was used to hold-

down the end studs by using a 600mm long box section stud (made from two stud sections to form a closed box shape) connected at the bottom of each end studs using 6 screws (12 gauge 30mm long Hex.Head Metal Tek[®]). As wall panels are isolated from the surrounding structure and tested in the laboratory, 6 screws are used in the test method to emulate the number of screws used in the Australian cold-formed steel-framed houses (bracing walls are connected with intersecting walls or unbraced continuous walls with a minimum of 2 screws each at top, bottom and noggin level but not more than 1350mm spacing, NASH 2014). These restraints were tied together horizontally along the length of the wall panel using 12mm dia. threaded rods. All CFS members were grade G550 and the connections between them were made using 15mm long M6 GX[®] Frame Screws. The sheathing boards were connected to the framing members at 100mm spacings along the periphery of the board and at 150mm spacings for the middle portion of the board. All sheathing screws were 20mm long M5-16TPI CSK FibreZips self drilling screws.

Two types of loading conditions were applied for the racking test; monotonic and cyclic loads. Monotonic loading was performed prior to the cyclic test to determine the displacement controlled parameter (Δ_M) which is a key parameter required for cyclic loading protocol (shown in Figure 1). Displacement controlled parameter (Δ_M) refers to the displacement corresponding to 90% of the peak strength at the declining portion of the monotonic load deflection curve. The cyclic loading protocol used in the testing program was slightly modified from the loading protocol developed by Shahi *et al.* (2013). According to this loading protocol, wall panel was first subjected to four cycles in Phase 1 with displacement amplitude of Δ_1 , where Δ_1 refers to serviceable displacement which corresponds to 8mm (H/300) for a 2.4m wall height. Second Phase of the loading protocol consisted of four cycles with displacement amplitude Δ_2 and three cycles each in Phase 3 and Phase 4 with displacement amplitudes of Δ_3 and Δ_4 respectively. Increment of the displacement amplitude in each subsequent cycle was kept uniform for simplicity which is given by the following expression:

$$\delta = (\Delta_M - \Delta_1)/3 \quad (1a)$$

where,

$$\Delta_M = \text{Displacement corresponding to 90\% of the peak strength at the declining portion of the monotonic load deflection curve}$$

After finding the incremental displacement δ , displacement amplitude at any loading phase (n) can be determined from following expression:

$$\Delta_n = \Delta_1 + (n - 1)\delta \quad (1b)$$

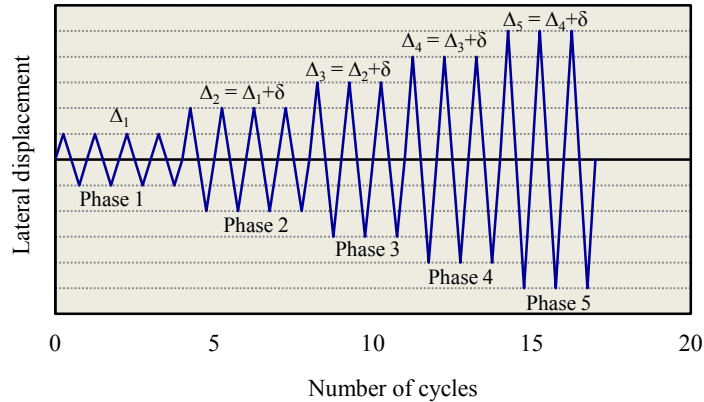


Figure 1 Modified cyclic loading protocol (Shahi *et al.* 2013)

All tests were conducted in the displacement controlled mode with a loading rate of 2 to 4mm/min for the monotonic tests and 4 to 16mm/min for the cyclic tests.

Table 1 Matrix of test specimen

Specimen	Loading	Length (L)	Height (H)	Stud Spacing	Aspect Ratio (H/L)	Number of boards
FCB-Mon-A	Monotonic	2.4m	2.4m	600mm	1.0	2
FCB-Mon-B	Monotonic	0.9m	2.4m	450mm	2.7	1
FCB-Cyc-A	Cyclic	2.4m	2.4m	600mm	1.0	2
FCB-Cyc-B	Cyclic	0.9m	2.4m	450mm	2.7	1

2.1 Monotonic test results

Load-deflection curves of the wall panels under monotonic loading are shown in Figure 2. The X-axis of Figure 2 represents the net racking displacement (after deducting rocking displacement) and the Y-axis represents the load carried by the wall panel. The general observations made from the monotonic load-deflection curves (Figure 2) are listed below:

- (a) FCB-Mon-A is found to be stiffer (about 30%) than the shorter panel FCB-Mon-B. The reason for the lower stiffness of the shorter wall panel (aspect

- ratio of 2.7) is the larger bending deformation which is not significant in the longer wall (with aspect ratio equal to 1).
- Nonlinear behavior in FCB-Mon-A starts at a load of around 60% of the ultimate load whereas nonlinearity starts at 40% of the ultimate load in the shorter panel FCB-Mon-B. The nonlinear behavior in both wall panels was mainly due to deformations at the fasteners which connect the CFS framing members with the sheathing board.
 - After reaching peak load, both wall panels undergo higher displacement without any further increase in load as illustrated by the plateau region in the load-deflection curve. This was primarily due to bearing of the fastener connections and screw head pull-through the sheathing board.
 - Both wall panels possessed similar load carrying capacity per unit length of wall panel. Hence, load carrying capacity of wall panels of intermediate lengths can be estimated using linear interpolations. However, deflection capacity of the shorter wall panel FCB-Mon-B was found to be 20% higher than the longer wall panel FCB-Mon-A.

Both wall panels ultimately failed by failure of the perimeter screws. Important parameters from the load-deflection curves (Figure 2) such as peak strength, deflection at peak strength, deflection at 90% of peak strength (Δ_M to be utilized in cyclic loading protocol) are provided in Table 2.

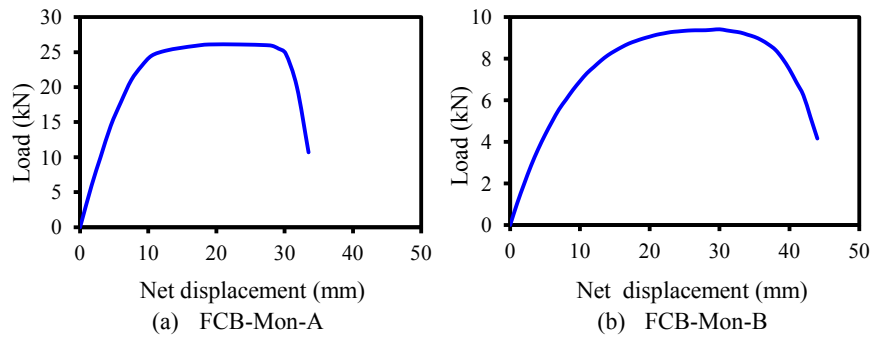


Figure 2 Load deflection behavior of wall panels under monotonic loading

Table 2 Summary of monotonic test results

Specimen	Displacement Controlled Parameter Δ_M (mm)	Peak Load S_{Peak} (kN)	Net racking displacement at Peak Load Δ_{Peak} (mm)
FCB-Mon-A	30	26.1	23.4
FCB-Mon-B	37	9.4	27.9

2.2 Cyclic test results

Hysteretic behavior of the wall panels under cyclic tests for FCB-Cyc-A and FCB-Cyc-B are shown in Figures 3a and 3b respectively. The X-axis of Figures 3a and 3b represents the net raking displacement. The load-deflection hysteresis of both wall panels showed severely pinched loops with large residual displacement (displacement corresponding to zero load while unloading). This reflects that bearing of the fastener into the sheathing material was the primary mode of resistance. Important parameters such as peak load and residual displacement were obtained for the virgin and last cycles at each phase of loadings which are summarized in Table 3. These parameters were obtained from the average of positive and negative hysteresis loops. The load carrying capacity was degraded from the virgin cycle to the last cycle of loading at the same displacement amplitude (same phase) which is referred herein as 'load degradation'. For both wall panels, the test results showed a load degradation of less than 10% at first phase of loading, 15 to 30% at second and third phases of loading and a severe load degradation (about 50%) at final phase of loading. The residual displacement after each cycle is a function of the maximum displacement at that cycle. Results shown in Table 3 for both wall panels showed a reasonably constant residual displacement ratio; 0.31 to 0.37 before reaching peak loads and 0.45 to 0.50 for cycles post the peak load. The residual displacement is an important parameter in evaluating wall performance and should not exceed the wall plumb line tolerance limit at serviceability limit state. The residual displacement at serviceability limit state (at displacement of H/300) of the tested wall panels satisfied the tolerance limit set by the NASH Standard, Australia (2005).

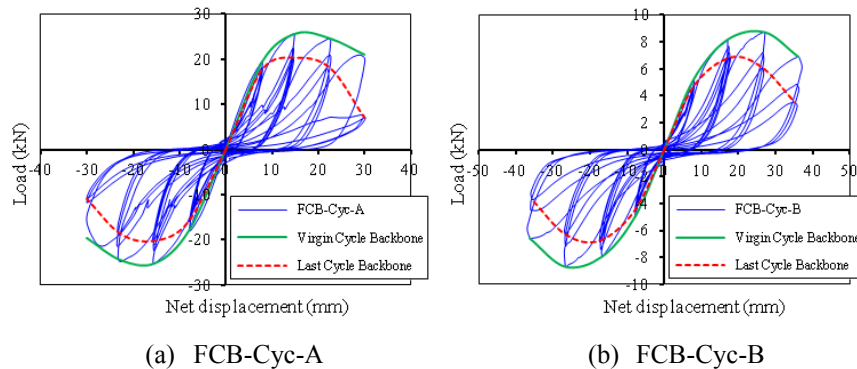


Figure 3 Load-deflection behavior of the wall panels under cyclic loading

Table 3 Summary of cyclic test results

Specimen	Loading Phase	Net racking disp. Δ (mm)	Test Load (kN)		Load Degra.	Maximum Residual Disp. Δ_R (mm)	Δ_R/Δ
			Virgin Cycle (P)	Final Cycle (R)			
FCB-Cyc-A	1	8.0	18.8	16.9	10%	2.5	0.31
	2	15.3	25.4	20.3	20%	5.7	0.37
	3	22.7	24.5	18.4	25%	10.2	0.45
	4	30.0	21.2	8.6	59%	15.0	0.50
FCB-Cyc-B	1	8.0	5.1	4.6	9%	2.7	0.34
	2	17.7	8.0	6.8	16%	6.1	0.35
	3	27.3	8.7	6.2	29%	12.9	0.47
	4	37.0	6.7	3.6	46%	17.5	0.47

Note: Values shown in above table are average values. While calculating average, any value in excess of 20% of the lowest value is discarded

3. Evaluation of Wall Parameters

Determination of important wall parameters such as stiffness, yield displacement, ultimate displacement and ductility are not easy in the cases of CFS wall panels since the load-deflection curve is highly non-linear. There are different methodologies for establishing the yield displacement and the equivalent bilinear backbone curve from the observed nonlinear load-deflection backbone curve; some of them are illustrated in Figure 4. According to test methods developed in New Zealand (P21 1988 and EM3 2000), the initial stiffness is the secant stiffness obtained by joining the origin to a value of 0.5 or 0.6 times the maximum strength along the backbone curve (shown in Figures 4a and 4b). The yield point is the intersection of initial stiffness and a horizontal line passing through the maximum strength whereas other models (AISI 2007 and Kawai *et al.* 1997) were based on the Equivalent Energy Elastic-Plastic (EEEP) principle. Kawai *et al.* model use the drift angle (drift ratio of 1/400 (Δ_{400})) for determining the initial stiffness whereas AISI standard use the strength ($0.4 R_{Peak}$) as in the cases of P21 and EM3 models. Unlike EM3 and P21 models, the limit state in both AISI and Kawai models are selected in such a way that the dissipated energy by the wall specimen during monotonic or cyclic load is equivalent to the energy represented by the bilinear system (as illustrated by the hatched area of Figures 4c and 4d). Structural ductility factor is the ratio of ultimate displacement (Δ_u) to yield displacement (Δ_y) in all models. Determination of ultimate displacement for all models is explained below:

- (a) P21 model: Ultimate displacement is set at $5\Delta_s$ where Δ_s is the serviceable displacement which is equal to $H/300$ and H is the height of specimen.
- (b) EM3 model: Ultimate displacement is the displacement corresponding to 90% of strength at the declining portion of the back bone curve and should not be greater than 35 mm for maintaining displacement compatibility with other bracing wall panels used in the structure.
- (c) AISI Standard: Ultimate displacement is the displacement corresponding to 80% of strength at the declining portion of the back bone curve.
- (d) Kawai *et al.* model: Ultimate displacement is the intersection of the horizontal yield line to the declining portion of the back bone curve. This involves several trials until the two hatched areas (Figure 4d) are equal.

Performance parameters of the wall panels obtained from cyclic (last-cycle) load-deflection backbone curves using different models are provided in Table 4. These values are obtained from the average of positive and negative last-cycle backbone curves. While calculating average, any value in excess of 20% of the lowest value is discarded. The general observations of various wall parameters using different models are listed below:

- (a) There was a slight variation in the initial stiffness (K) of wall panels obtained from all four models, with AISI Standard giving slightly higher values.
- (b) Similarly, there was a marginal variation in the ultimate strength (R_u) of wall panels obtained from all considered models. Ultimate strengths obtained from P21 and EM3 models were slightly higher compared to other two models since these models used peak loads as the ultimate loads from the backbone curves. Ultimate strengths obtained from EEEP models (AISI Standard and Kawai *et al.*) were found to be in between 80 and 100% of peak load with AISI Standard giving slightly lower value.
- (c) Yield displacement (Δ_y) was computed based on drift angle in Kawai *et al.* model unlike other models which were based on fractions of peak load. Yield displacement obtained from AISI Standard was found to be smallest compared to other models which is due to high initial stiffness as discussed above.
- (d) The largest ultimate displacement (Δ_u) was observed in P21 model which was due to the ultimate displacement (Δ_u) deliberately set at 5 times the serviceable displacement and is found to be extremely larger for the considered wall panels compared to other models. Whereas, the smallest ultimate displacement was observed in Kawai *et al.* model as the horizontal yield line (ultimate strength) intersected the declining portion of the backbone curve at the value greater than 90% of peak load for the considered wall panels. i.e. In the declining portion of the back bone curve,

Δ at load greater than 90% of peak load (Kawai *et al.* model) $< \Delta$ at 90% of peak load (EM3 model) $< \Delta$ at 80% of peak load (AISI Standard).

- (e) Structural ductility factors and energy absorptions under equivalent elasto-plastic curves are highly dependent on the ultimate displacement (as the ultimate strengths from all models were found to be similar). Similar to the ultimate displacement, structural ductility factors and energy absorptions obtained from P21 and Kawai *et al.* models were found to be largest and smallest respectively amongst all considered models.

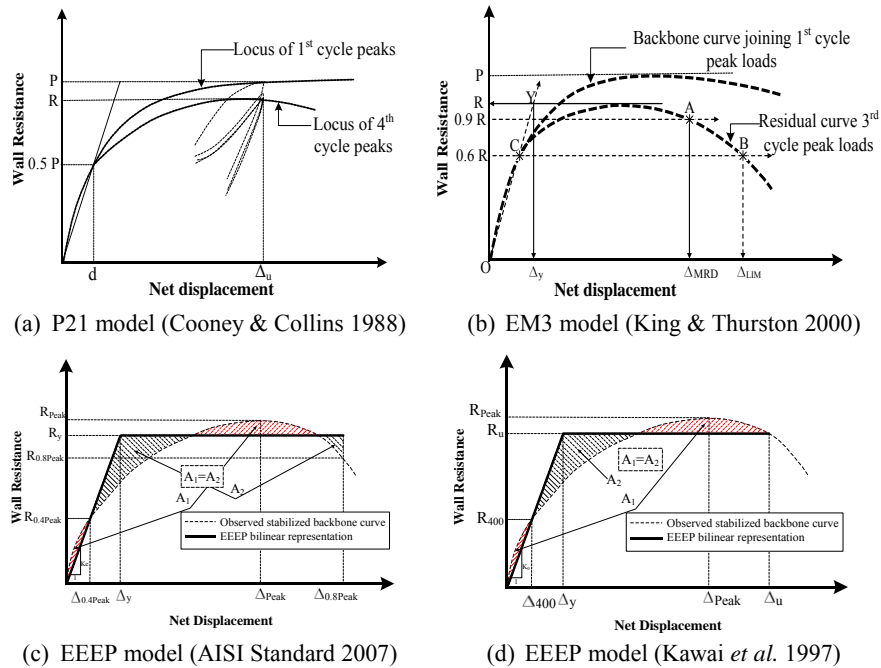


Figure 4 Determination of yield points using different methods

Based on the above comparisons, it can be concluded that EEEP models (AISI Standard and Kawai *et al.*) are reasonable for computing ultimate strength compared to P21 and EM3 models. Both P21 and EM3 models considered full strength which is not necessary that the wall panels possess same level of strength at ultimate displacement. There are two major differences between AISI Standard and Kawai *et al.* models; definition of initial stiffness and ultimate displacement. Kawai *et al.* model use the drift angle for defining the initial stiffness which has the beauty to control the response of specimen in terms of

displacement rather than force. Hence the authors propose to use the drift angle to define the initial stiffness. However, Kawai *et al.* model significantly compromised the value of ultimate displacement for a slight increase in ultimate load compared to AISI Standard. This results in lower displacement capacity as well as structural ductility factor. Hence, the authors propose the use of a slightly modified version from both models, i.e. considering the drift angle from Kawai *et al.* model and the definition of ultimate displacement from the AISI Standard which is simple and effective compared to Kawai *et al.* model.

Table 4 Performance parameters of wall panels using different methods

Specimen	Backbone Curve	Wall Parameters	P21 Model	EM3 Model	AISI Standard	Kawai <i>et al.</i> Model	Proposed Model
FB-Cyc-A	Last-cycle (Average of positive and negative cycles)	K	2.60	2.80	2.88	2.41	2.41
		R_u	20.1	20.1	18.8	20.0	19.4
		Δ_y	7.8	7.2	6.5	8.3	8.1
		Δ_u	23.0	41.0	25.3	19.5	25.3
		μ	3.0	5.7	3.9	2.3	3.1
		Energy	384	753	412	307	412
FB-Cyc-B	Last-cycle (Average of positive and negative cycles)	K	0.55	0.58	0.61	0.58	0.58
		R_u	7.0	7.0	6.4	6.5	6.5
		Δ_y	12.6	12.1	10.5	11.3	11.3
		Δ_u	27.3	41.0	30.1	26.5	30.1
		μ	2.2	3.4	2.9	2.4	2.7
		Energy	146	244	159	136	159

K = Initial stiffness (kN/mm), R_u = Ultimate strength (kN), Δ_y =Yield displacement (mm), Δ_u = Ultimate displacement (mm), μ = Structural ductility factor, and Energy = Energy absorption under equivalent elasto-plastic curve (Joules)

Note: Values shown in above table are average values. While calculating average, any value in excess of 20% of the lowest value is discarded

4. Bracing rating of wall panel

Unlike other methods, P21 and EM3 methods consider several other parameters such as ductility modification factor, residual displacement recovery, displacement compatibility and asymmetry of performance while calculating bracing rating (capacity) of wall panels. This study considered the basis of the New Zealand test methods for evaluating bracing rating of wall panels against earthquake loading. The design bracing rating of wall panels for earthquake loading is obtained from the last-cycle backbone curve and it should satisfy ultimate as well as serviceability limit state conditions.

(i) Earthquake resistance at ultimate limit state is given by

$$EQ_u = K_1 * R_u / K_t \quad (2a)$$

where,

K_1 = Ductility modification factor

R_u = Average ultimate strength from last-cycle backbone curve (Proposed model in Table 4)

K_t = Sampling factor which depends on the variations of production units due to fabrication and material. NASH Standard (NASH 2005) specifies a minimum of 15% of coefficient of variations for sub assembly tests. According to Amendment C of NASH Standard (NASH 2005), $K_t = 1.79$ for 1 sample tested with 15% coefficient of variation

The ultimate resistance of wall panel to earthquake load is factored by ductility modification factor K_1 so that it represents an equivalent structural ductility factor of 3.0. The ductility modification factor is obtained by suppressing the yield displacement maintaining same elastic stiffness and ultimate displacement as shown in Figure 5. A modification is not required if the structural ductility factor of the tested wall panel is equal to or greater than 3. However, wall panels with ductility modification factor less than 0.5 are deemed to be considered as unstable and no rating will be made.

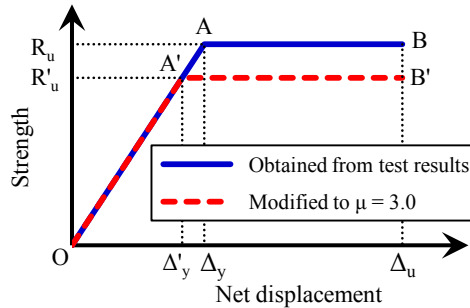


Figure 5 Determination of ductility modification factor

From Figure 5,

$$\triangleright K_1 = \frac{R'_u}{R_u} = \frac{K * \Delta'_y}{K * \Delta_y} = \frac{\Delta u / \mu'}{\Delta u / \mu}$$

$$\triangleright K_1 = \mu / \mu'; (0.5 \leq K \leq 3.0) \quad (2b)$$

where,

$\mu = \Delta_u/\Delta_y$ = Average structural ductility factor for last-cycle equivalent elasto-plastic curve (from Proposed model in Table 4)

$\mu' = \Delta_u/\Delta'_y$ = Structural ductility factor modified to a value of 3.0

(ii) Earthquake resistance at serviceability limit state is given by

$$EQ_s = K_2 * R_s * LR_{EQ} / K_t \quad (3a)$$

where,

K_2 = Displacement recovery factor

R_s = Average test load from last-cycle backbone curve at serviceable displacement ($\Delta_s = H/300 = 8\text{mm}$) which is provided in Table 3

LR_{EQ} = Load ratio for earthquake loading

Displacement recovery factor K_2 is specified to allow for any residual (non-recoverable) displacement at the serviceability loading cycles, thereby restricting the unnecessary permanent offset. NASH Standard, Australia (NASH 2005) specifies the tolerance limit of $H/600$ or 3mm whichever is greater. Hence, the average residual displacement of wall panels at serviceability loading cycles must not exceed the specified tolerance limit. A moderate level of residual displacement is allowed in the evaluation method with the residual displacement not exceeding 30% of the serviceable displacement. If the residual displacement (Δ_R) exceeds 30% of the serviceable displacement (Δ_s), then the rated load is reduced by using following expression:

$$K_2 = .3 - \frac{\Delta_R}{\Delta_s}; (0.8 \leq K_2 \leq 1.0) \quad (3b)$$

where,

Δ_R = Residual displacement during serviceability displacement ($\Delta_s = H/300 = 8\text{mm}$) loading cycle which is provided in Table 3

Load ratio for earthquake loading is the ratio of equivalent base shear at ultimate and serviceability limit states. The equivalent static base shear as per Australian Standard AS 1170.4:2007 is given by:

$$V = [k_p Z C_h(T_1) S_p / \mu] W_t \quad (3c)$$

where,

k_p = Probability factor = 1.0 for 500 year return period (ultimate limit state) and 0.25 for 25 year return period (serviceability limit state)

Z = Hazard factor

$C_h(T_1)$ = Value of spectral shape for the fundamental natural period of the structure

S_p = Structural performance factor

μ = Structural ductility factor

W_t = Seismic weight of the structure

Considering the structural ductility factor (μ) of 1 at serviceability limit state (25 year return period) and 3 at ultimate limit state (500 year return period), load ratio for earthquake loading is computed as:

$$LR_{EQ} = \frac{\{[k_p Z C_h(T_1) S_p / \mu] W_t\} \text{ at ultimate limit state}}{\{[k_p Z C_h(T_1) S_p / \mu] W_t\} \text{ at serviceability limit state}} \quad (3d)$$

$$= \frac{[k_p / \mu] \text{ at ultimate limit state}}{[k_p / \mu] \text{ at serviceability limit state}} = \frac{[1.0/3]}{[0.25/1]} = 1.33$$

The bracing ratings of the tested wall panels for earthquake loading are computed using equations 2 to 3 and are provided in Table 5.

Table 5 Bracing ratings of tested wall panels for earthquake loading

Bracing Rating	Parameters	Wall Specimen		References
		FCB-Cyc-A	FCB-Cyc-B	
ULS	μ	3.10	2.70	Table 4 (Proposed model)
	K_1	1.00	0.90	Eq.2b: $K_1 = \mu / \mu'$; (0.5 K_2 .0) ($\mu' = 3.0$)
	R_u (kN)	19.40	6.50	Table 4 (Proposed model)
	K_t	1.79	1.79	NASH 2005 (for $N=1$ & $CoV=15\%$)
	EQ_u (kN)	10.84	3.27	Eq.2a: $K_1 * R_u / K_t$
SLS	Δ_R (mm)	2.50	2.70	Table 3
	Δ_s (mm)	8.00	8.00	$H/300$ ($H=2400\text{mm}$)
	K_2	0.99	0.96	Eq.3b: $K_2 = 1.3 - \Delta_R / \Delta_s$; (0.8 K_1 .0)
	R_s (kN)	16.90	4.60	Table 3 (Last cycle load at Δ_s)
	K_t	1.79	1.79	NASH 2005 (for $N=1$ & $CoV=15\%$)
	LR_{EQ}	1.33	1.33	Eq.3d
	EQ_s (kN)	12.43	3.28	Eq.3a: $EQ_s = K_2 * R_s * LR_{EQ} / K_t$
Design capacity per unit length (kN/m)		4.52	3.63	Minimum of EQ_u and EQ_s divided by the length of wall panel

5. Summary and Conclusions

This paper presented experimental test results of cold-formed steel-framed bracing wall panels braced with fibre cement board as sheathing material, subjected to in-plane monotonic and cyclic loadings. Four panels of different aspect ratios were tested under monotonic and cyclic loadings. A new loading protocol which had been recently developed based on the seismic conditions of Australia was used for cyclic testing. Monotonic test results of the tested wall panels showed similar load carrying capacity per unit length of wall panel. However, the deflection capacity of the wall panel with shorter length (or larger aspect ratio) was found to be 20% higher than the wall panel with aspect ratio of 1. Cyclic test results showed a severely pinched hysteresis associated with both stiffness and load degradations. Test results showed a load degradation of less than 10% at the serviceability displacement loading whereas severe load degradation (about 50%) was observed after post peak loading for both wall panels. Residual displacement ratios for both wall panels were found to be constant; 0.31 to 0.35 before reaching peak loads and 0.45 to 0.50 for cycles post the peak load.

Various existing methods were used for the evaluation of wall parameters from the observed last-cycle load-deflection backbone curves. Initial stiffness and ultimate strength of the wall panels obtained from all methods were found to be consistent with each other, with AISI Standard model giving slightly higher stiffness and P21 and EM3 models giving slightly higher ultimate strength. However, structural ductility factor from P21 model was found to be significantly higher compared to other methods. The authors propose the evaluation method with slight modifications from the existing AISI Standard and Kawai *et al.* models which were based on Equivalent Energy Elastic-Plastic (EEEP) principle. The evaluation method considered other parameters including displacement modification factor, residual displacement recovery, sampling factor and load levels satisfying serviceability as well as ultimate limit states, while determining bracing rating of wall panels under earthquake loading.

Acknowledgements

This research is funded by ARC Linkage Project LP110100430. The authors gratefully acknowledge the financial and technical support provided by the collaborating organization, the National Association of Steel-framed Housing (NASH). Supply of materials and technical data by NASH members is also gratefully acknowledged.

References

- AISI S213-07 (2007). North American standard for cold-formed steel framing-lateral design. American Iron and Steel Institute, USA.
- AS 70.4 (007). Australian Standard, Structural design actions–Part 4: Earthquake actions in Australia.
- Cooney R.C. and Collins M.J. (1988). A wall bracing test and evaluation procedure. *Technical Paper P21*, Building Research Association of New Zealand (BRANZ), Judgeford, New Zealand.
- Gatto K. and Uang C. (2003). Effects of loading protocol on the cyclic response of woodframe shearwalls. *Journal of Structural Engineering, ASCE*, 129(10):1384-1393.
- Kawai Y., Kanno R. and Hanya K. (1997). Cyclic shear resistance of light-gauge steel framed walls. *Proceedings in ASCE Structures Congress*, Poland, USA.
- King A.B. and Thurston S.J. (2000). EM3 wall bracing rating test and evaluation procedure. A Background Paper, Judgeford, New Zealand.
- NASH Standard (2005). Residential and low-rise steel framing–Part : Design criteria. National Association of Steel-framed Housing Inc, Australia.
- NASH Standard (2014). Residential and low-rise steel framing–Part : Design solutions. Draft Standard, National Association of Steel-framed Housing Inc, Australia.
- Shahi R., Lam N., Gad E. and Wilson J. (2013). Protocol for testing of cold-formed steel wall in regions of low-moderate seismicity. *Earthquakes and Structure*, 4(6), 629-647.